Finite-Element Shock Analysis of an Operating Hard Disk Drive Considering the Flexibility of a Spinning Disk-Spindle, a Head-Suspension-Actuator, and a Supporting Structure

G. H. Jang and C. H. Seo

PREM, Department of Mechanical Engineering, Hanyang University, Seoul 133-791, Korea

This paper proposes a finite-element method (FEM) with mode superposition to analyze the shock response of a flexible hard disk drive (HDD) composed of a spinning disk-spindle system with fluid dynamic bearings (FDBs), a head-suspension-actuator with pivot bearings and air bearings, and a base plate with complicated geometry. The proposed method is applied to a 2.5-in HDD. The displacements of the head, spinning disk, and arm are calculated, and they are also measured by experiments. This research shows that the numerical results match well with the experimental ones. It also investigates the head-disk motion due to operational shock.

Index Terms—**Finite-element method (FEM), hard disk drive (HDD), head crash, mode superposition, operating shock.**

I. Introduction

SHOCK analysis of a hard disk drive (HDD) has been important in the HDD industry because severe vibration due to shock results in read/write error or head crash—a failure of the HDD in which the head scrapes across the platter surface, often grinding away the thin magnetic film. Shock characteristics of a HDD are determined by the dynamics of a HDD including the flexibility of the spinning disk-spindle, the head-suspension-actuator, the supporting structure and the fluid dynamic bearings (FDBs), ball and air bearings. A shock simulation model of a whole HDD including every component as shown in Fig. 1 has not yet been developed. One difficulty is that available commercial software cannot handle the spinning disk-spindle system including the flexibility of complicated supporting structure such as base and cover. The other difficulty is that the stiffness and damping coefficients of FDBs, ball bearing, and air bearing cannot be easily determined.

Many researchers have studied the dynamics or the shock response of a HDD by using various methods. One group of them has investigated the dynamics of disk, air bearing, and slider, and suspension assembly without considering the spinning disk-spindle system of a HDD itself. Shu *et al.* [1] studied the influence of the pulse width and pulse amplitude of half-sine acceleration pulse in a head actuator assembly with the finite-element method (FEM). Zeng and Bogy [2] investigated the shock response of an operational HDD using the finite-element model that includes the disk, suspension, slider, and air bearing. A finite-element model including the simplified base plate, the stationary disk, the actuator, the suspension, and the head was developed by Jayson *et al.* [3]. They did not consider the whole components of a HDD or the rotation of the disk-spindle system. Another group of researchers has investigated the dynamics of a rotating spindle system without considering air bearing and slider, suspension, and actuator assembly. Tseng

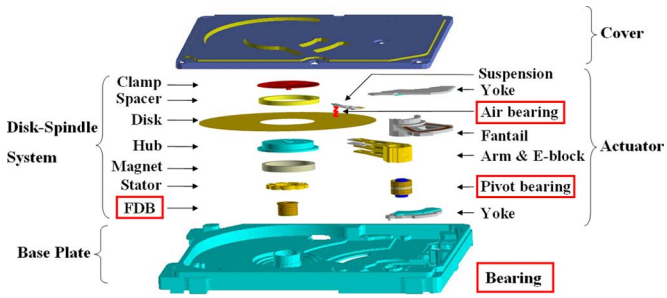

Fig. 1. Mechanical structure of a 2.5-in HDD.

et al. [4] proposed an analytical model of the HDD spindle system with FDBs including the flexibility of housing. They extracted several lower natural frequencies and mode shapes of the supporting structure of the HDD spindle system by using the FEM. The extracted mode shapes were applied to the HDD spindle system with rotating flexible disks to determine a set of equations of motion by using the Lagrange equation. Jang *et al.* [5] proposed a consistent method to predict the natural frequencies and mode shapes of a rotating disk-spindle system in the HDD with FDBs by accounting for the flexibility of a complicated supporting structure using the FEM and substructure synthesis. They derived the finite-element equations of each substructure of a HDD spindle system from the spinning flexible disk to the flexible base plate by ensuring the geometric compatibility in the internal boundary between each substructure. However, their model did not include the head-suspension-actuator or the air bearing between spinning disk and head. Recently, Jang *et al.* [6] developed a FEM to analyze the free vibration of a flexible HDD composed of the spinning disk-spindle system with FDBs, the head-suspension-actuator with air and pivot bearings, and the base plate with complicated geometry by using 3-D tetrahedral element and 2-D shell element appropriately.

This paper extends Jang's method [6] to analyze the shock response of a flexible HDD composed of the spinning disk-spindle system with FDBs, the head-suspension-actuator with air and pivot bearings, and the base plate with complicated geometry

Digital Object Identifier 10.1109/TMAG.2007.902981

Color versions of one or more of the figures in this paper are available online at http://ieeexplore.ieee.org.

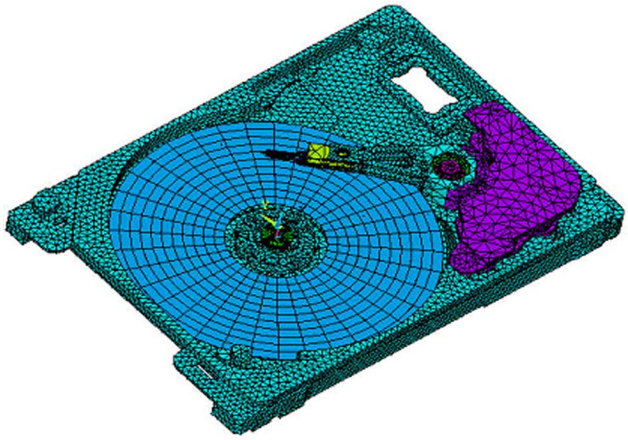

Fig. 2. Finite-element model of a 2.5-in HDD composed of the spinning disk-spindle, the head-suspension-actuator, and the base plate.

by using the mode superposition. The proposed method is applied to a 2.5-in HDD and the validity of the model is verified by comparing the numerical results with the experimental ones.

II. Method of Analysis

A. Finite-Element Modal Analysis

This paper follows Jang's method [6] to calculate the free vibration characteristics, i.e. the natural frequencies, ω_i and the mode vectors, $\boldsymbol{\phi}_i$ of a flexible 2.5-in HDD at 5400 rpm as shown in Fig. 2. It is composed of a spinning disk-spindle system with FDBs, a head-suspension-actuator with air and pivot bearings, and a base plate with complicated geometry. It uses annular sector elements for the spinning disk, beam elements for the spindle and shaft, and 4-node tetrahedral elements with rotational degrees of freedom for the base plate. The hinge, flexure, and load beam of the actuator are discretized by 4-node shell elements with rotational degrees of freedoms, and the 2-D shell elements are connected to the 3-D tetrahedral elements of the actuator arm in such a way to satisfy the requirement of the geometric compatibility. The FDBs of the spindle motor are modeled by the five linear spring elements with damper, and the pivot bearings of the actuator are modeled by the linear spring elements. The air bearing between spinning disk and head is modeled by the axial linear spring element. The effect of the suspension preload is replaced by a linear spring. The head is assumed to be connected to the dimple. The complete description of the finite-element model and a comparison of its natural frequencies and mode shapes with the experimental results are given in [6].

The global finite-element equation can be expressed as follows:

$$\mathbf{M}\ddot{\mathbf{u}} + (\mathbf{C}+\mathbf{G})\dot{\mathbf{u}} + \mathbf{K}\mathbf{u} = \mathbf{0} \tag{1}$$

where $\mathbf{M}$, $\mathbf{G}$, $\mathbf{C}$, and $\mathbf{K}$ are the mass, gyroscopic, damping, and stiffness matrices of the global finite-element equation, respectively. Equation (1) is transformed to a state-space form as follows:

$$\lambda \begin{bmatrix} -\mathbf{G}-\mathbf{C} & -\mathbf{M} \\ \mathbf{M} & \mathbf{0} \end{bmatrix} \begin{Bmatrix} \mathbf{x} \\ \lambda\mathbf{x} \end{Bmatrix} = \begin{bmatrix} \mathbf{K} & \mathbf{0} \\ \mathbf{0} & \mathbf{M} \end{bmatrix} \begin{Bmatrix} \mathbf{x} \\ \lambda\mathbf{x} \end{Bmatrix}. \tag{2}$$

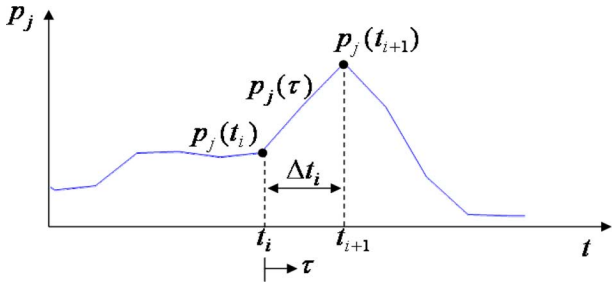

Fig. 3. Linear interplolation of the excitation force.

The restarted Arnoldi iteration method [7] is applied to solve the large, asymmetric eigenvalue problem to determine the natural frequencies and mode shapes of the finite-element model.

B. Finite-Element Shock Analysis

The equations of motion with the excitation force $\mathbf{Q}$ can be represented by the following state space equation:

$$\begin{bmatrix} \mathbf{C}+\mathbf{G} & \mathbf{M} \\ -\mathbf{M} & \mathbf{0} \end{bmatrix} \begin{bmatrix} \dot{\mathbf{u}} \\ \ddot{\mathbf{u}} \end{bmatrix} + \begin{bmatrix} \mathbf{K} & \mathbf{0} \\ \mathbf{0} & \mathbf{M} \end{bmatrix} \begin{bmatrix} \mathbf{u} \\ \dot{\mathbf{u}} \end{bmatrix} = \begin{bmatrix} \mathbf{Q} \\ \mathbf{0} \end{bmatrix}$$
$$\text{or } \mathbf{M}^*\dot{\mathbf{r}} + \mathbf{K}^*\mathbf{r} = \mathbf{Y}. \tag{3}$$

The forced response can be approximated with the lowest 2n modes with complex number

$$\mathbf{r}(t) = \sum_{j=1}^{2n} z_j(t)\boldsymbol{\phi}_j = \boldsymbol{\Phi} z(t). \tag{4}$$

Equation (4) is substituted into (3). Then, the 2n equations of motion can be obtained after multiplying (3) by $\boldsymbol{\Phi}^T$ with the assumption that the asymmetric terms of the stiffness and damping matrices from FDBs and the gyroscopic matrix play little effect on the global equation of motion of (1)

$$m_j\dot{z}_j + k_j z_j = p_j \quad (j = 1, 2, \ldots, 2n). \tag{5}$$

Fig. 3 shows the linear interpolation of the excitation force $p(t)$, and the decoupled equation of motion between t_i and t_{i+1} can be written as follows [8]:

$$m_j\dot{z}_j(\tau) + k_j z_j(\tau) = p_j(t_i) + \frac{p_j(t_{i+1}) - p_j(t_i)}{\Delta t_i}\tau. \tag{6}$$

With the given initial condition of $z_j(0) = z_j(t_i)$, the solution of (6) can be calculated, and then $z_j(t_{i+1})$ can be determined as follows:

$$z_j(t_{i+1}) = z_j(t_i)e^{-\frac{k_j}{m_j}\Delta t_i} + Ap_j(t_i) + Bp_j(t_{i+1}) \tag{7}$$

$$A = \frac{1}{\Delta t_i}\frac{m_j}{k_j^2} - \frac{1}{k_j}e^{-\frac{k_j}{m_j}\Delta t_i} - \frac{1}{\Delta t_i}\frac{m_j}{k_j^2}e^{-\frac{k_j}{m_j}\Delta t_i} \tag{8}$$

$$B = \frac{1}{k_j} - \frac{1}{\Delta t_i}\frac{m_j}{k_j^2} + \frac{1}{\Delta t_i}\frac{m_j}{k_j^2}e^{-\frac{k_j}{m_j}\Delta t_i}. \tag{9}$$

The displacement $z_j(t)$ is determined by using the above equation successively, and the forced response $\mathbf{r}(t)$ can be obtained from (4).

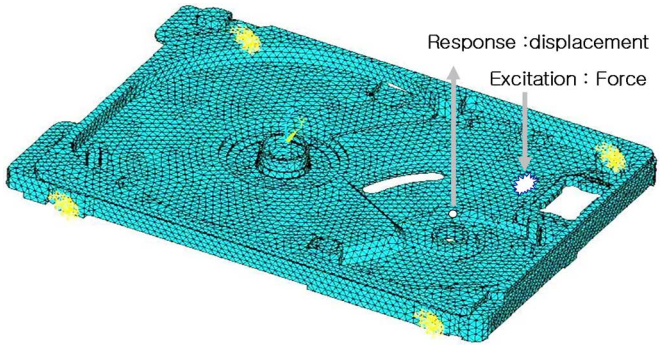

Fig. 4. Finite-element model of the base plate of a 2.5-in HDD.

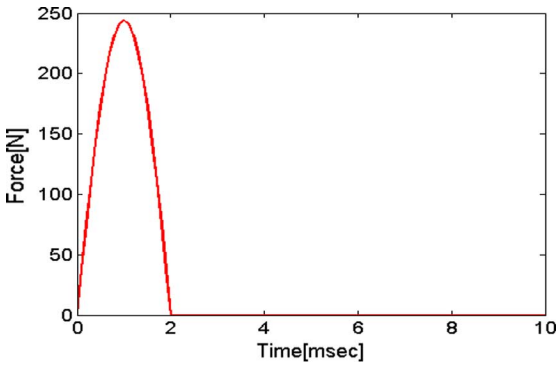

Fig. 5. Half-sinusoidal shock with the duration of 2 ms.

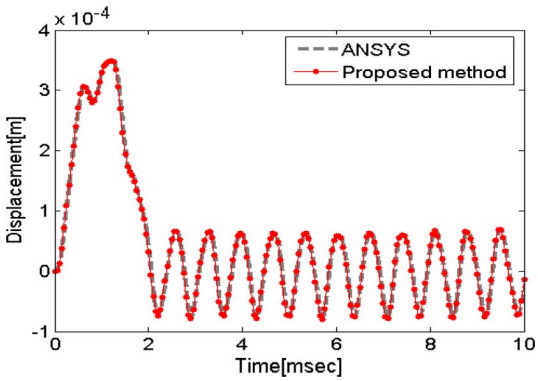

Fig. 6. Transient response calculated by the proposed method and ANSYS.

III. Result and Discussion

A. Verification I: Base Plate

The transient response of the proposed method is applied to the base plate of a 2.5-in HDD and is compared with that of a commercial software ANSYS. Fig. 4 shows a finite-element model of the base plate, the application point of the excitation force, and the calculated point of the response. A half-sinusoidal shock with a period of 2 ms is applied to the base plate in the $+z$ direction as shown in Fig. 5 and the transient response is calculated by the proposed method and the ANSYS, respectively. The motion is superposed with the lowest 15 modes. Fig. 6 shows the transient responses of the proposed method and the ANSYS. Transient response of the proposed method exactly agrees with that of the ANSYS, and it verifies that the numerical algorithm of the proposed method is theoretically valid.

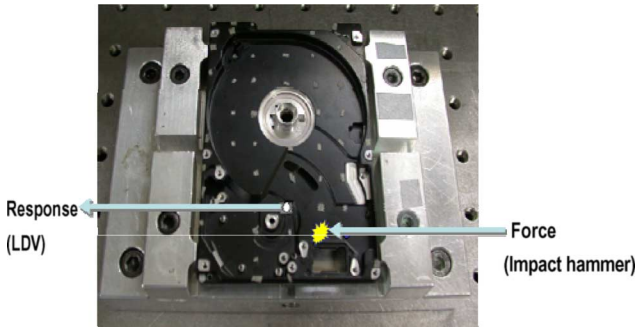

Fig. 7. Base plate fixed to the jig, and the application point of the excitation force and the measured point of the response.

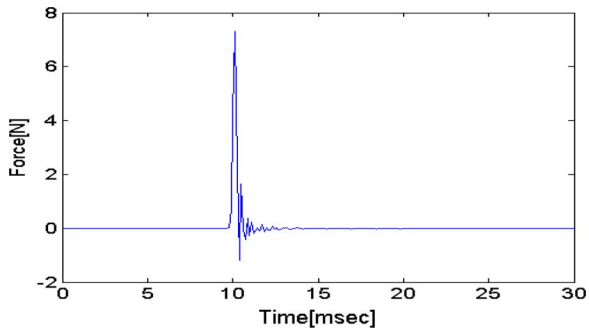

Fig. 8. Measured excitation force of the impact hammer.

Experimental testing is also performed to validate the proposed numerical method. Fig. 7 shows the base plate fixed to the jig, the application point of the excitation force, and the measured point of the response. The base plate of a 2.5-in HDD is fixed to the jig by screws. An impact hammer is used to excite the HDD and the response of the displacement is measured with a laser Doppler vibrometer. The excitation force of the impact hammer is measured as shown in Fig. 8 and the measurement is applied to the proposed numerical method to calculate the transient response. In the simulation, the motion is superposed with the lowest 130 modes. Figs. 9 and 10 are the measured and the simulated displacement, respectively. The simulated displacement does not damp because simulation model does not have any damping mechanism. On the other hand, the experimental model has damping mechanisms even though it may be mathematically indefinable. The simulated initial peak displacements, however, match well with the experimental ones (within 10%) as shown in Table I because the damping effect is minimal at the early stage of excitation. The proposed method may be effectively applied to predict the initial peak displacement of a HDD due to excitation.

B. Verification II: Spinning Disk-Spindle, Head-Suspension-Actuator, and Base Plate

Fig. 11 shows the spinning disk-spindle, the head-suspension-actuator, and the base plate of a 2.5-in HDD fixed to the jig. An impact hammer is used to excite the base plate of the HDD and its magnitude is measured with a force transducer. The displacement of the spinning disk, head, and arm are measured with a laser Doppler vibrometer. One excitation force and one displacement are measured at each experiment. Fig. 12 shows

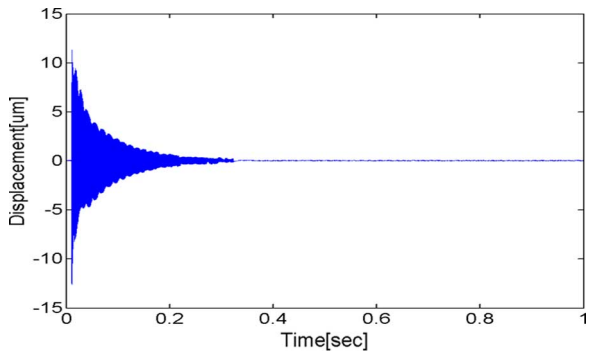

Fig. 9. Measured displacement of the base plate.

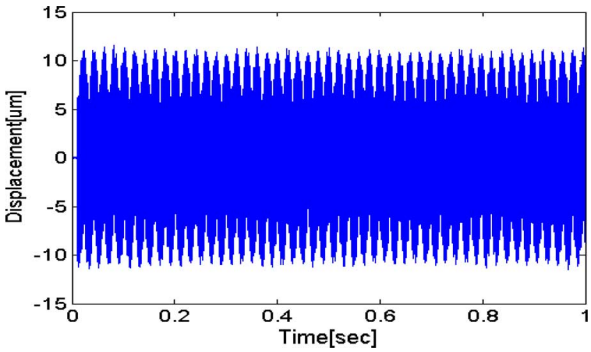

Fig. 10. Simulated displacement of the base plate.

TABLE I
COMPARISON BETWEEN EXPERIMENTAL AND SIMULATED MAXIMUM AND MINIMUM DISPLACEMENT OF THE BASE PLATE

	Experiment	Simulation	Error (%)
Maximum (μm)	11.28	11.63	3.06
Minimum (μm)	-12.64	-11.47	-9.26

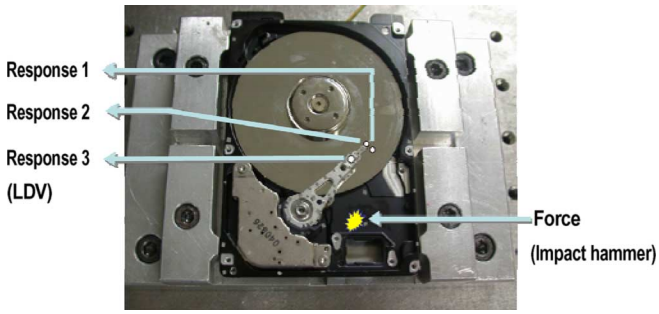

Fig. 11. Spinning disk-spindle, head-suspension-actuator, and base plate of the 2.5-in HDD fixed to the jig.

the excitation force used for each experiment. Three different excitation forces of the impact hammer in Fig. 12 are applied to the proposed method and the transient responses are calculated in each simulation. In the simulation, the motion is superposed with the lowest 130 modes.

1) Transient Response of the Spinning Disk (Response 1): Fig. 13 shows the measured transient displacement of the spinning disk (Response 1). Repeatable run-out (RRO) always exists in the HDD spindle system, and the pure vibration due to

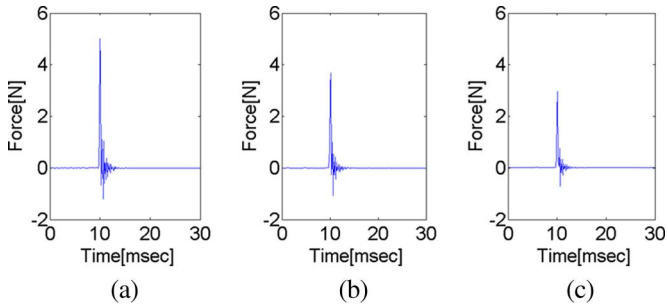

Fig. 12. Measured excitation force of the impact hammer for the response of the (a) spinning disk, (b) head, and (c) arm.

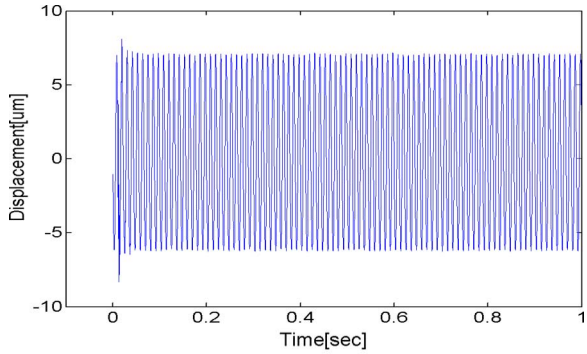

Fig. 13. Measured displacement of the spinning disk.

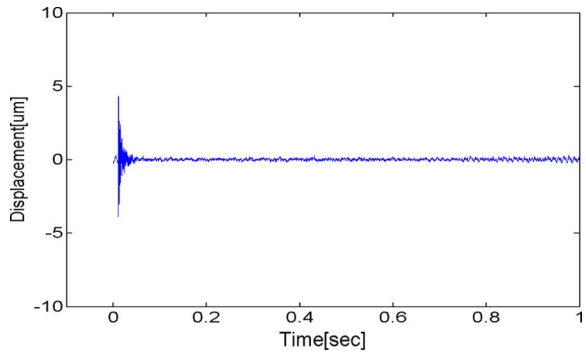

Fig. 14. Measured displacement of the disk after removing the RRO.

the excitation of impact hammer is the displacement without RRO. Fig. 14 shows the pure vibration due to excitation after RRO has been removed from the experimentally measured displacement. Fig. 15 shows the simulated displacement and it matches well with the measured one (within 7%) as shown in Table II. The FDBs damps out the simulated transient response but more slowly than the measured one does because the proposed method only includes the damping of the FDBs. But a real HDD has mathematically indefinable damping mechanisms such as air damping, structural damping, etc., in addition to the FDBs.

2) Transient Response of the Head (Response 2): Fig. 16 shows the measured transient displacement of the head (Response 2) after RRO has been subtracted from the experimentally measured displacement. The head motion exhibits significant amount of RRO because it follows the disk motion through air bearing. Fig. 17 shows the simulated displacement and its

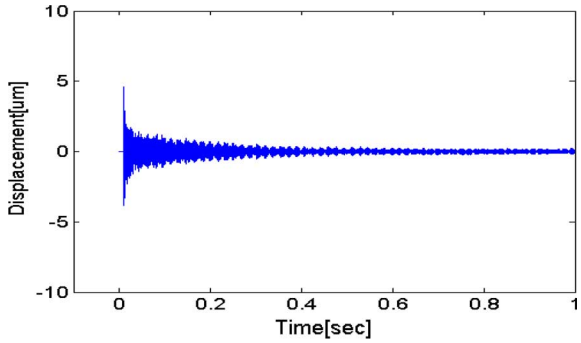

Fig. 15. Simulated displacement of the spinning disk.

TABLE II
COMPARISON BETWEEN MEASURED AND SIMULATED DISPLACEMENT OF THE SPINNING DISK, THE HEAD, AND THE ARM

Response		Experiment	Simulation	Error (%)
Spinning disk	Maximum (μm)	4.32	4.60	6.53
	Minimum (μm)	-3.91	-3.86	-1.34
Head	Maximum (μm)	2.52	2.56	1.69
	Minimum (μm)	-2.63	-2.76	4.90
Arm	Maximum (μm)	7.02	7.73	10.17
	Minimum (μm)	-8.62	-8.18	-5.11

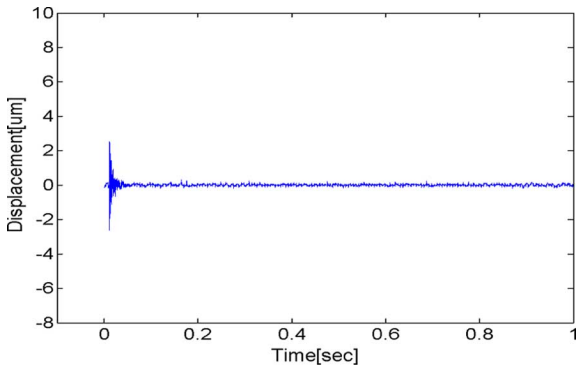

Fig. 16. Measured displacement of the head after removing the RRO.

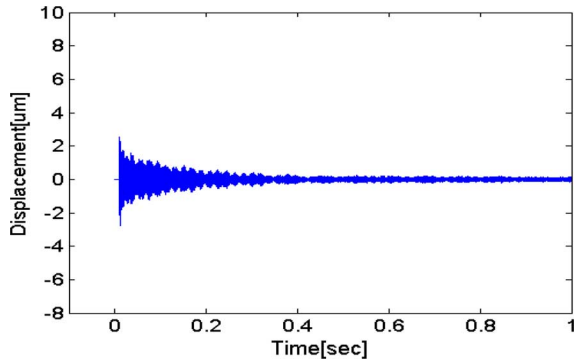

Fig. 17. Simulated displacement of the head.

peak value matches well with the measured one (within 5%) as shown in Table II. The FDBs damps out the simulated transient response, but again more slowly than the measured one does.

3) Transient Response on the Arm (Response 3): Fig. 18 shows the measured transient displacement of the arm (Response 3). Fig. 19 shows simulated displacement and it matches well with the measured one (within 11%) as shown in Table II. Damping of FDBs damps out the simulated transient response, but again more slowly than the measured one does. However, the proposed method predicts well the peak value of the displacement during the transient period.

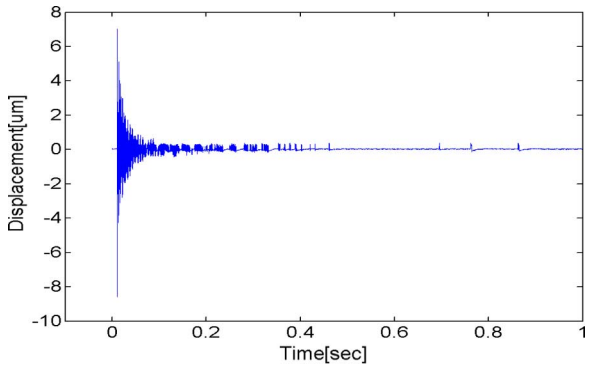

Fig. 18. Measured displacement of the arm.

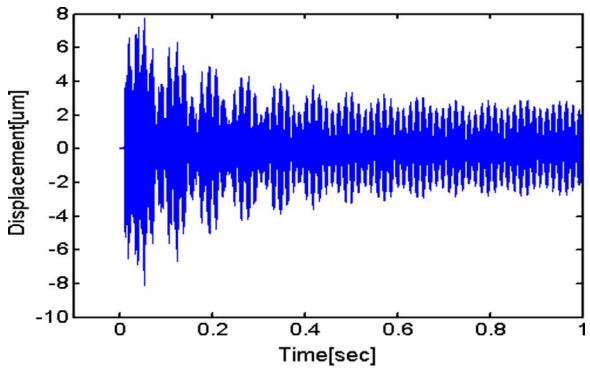

Fig. 19. Simulated displacement of the arm.

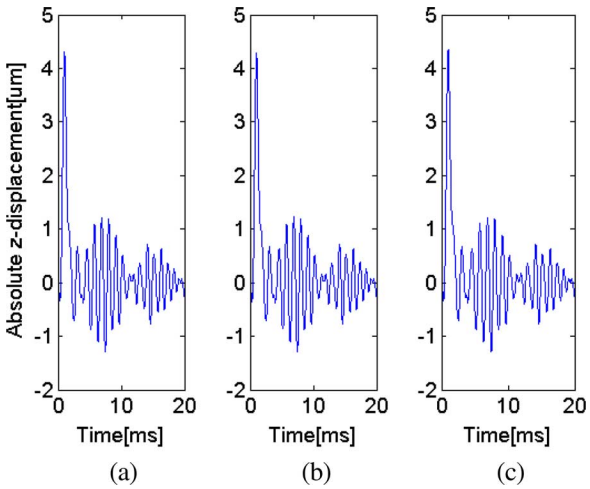

Fig. 20. Absolute displacement of (a) top head, (b) connecting point of disk, and (c) bottom head under the half-sinusoidal shock with the amplitude of 350 G and the duration of 2 ms.

C. Head-Disk Motion Due to the Change of Shock Amplitude

Head-disk motion is simulated due to the change of shock amplitude. It assumes that the half-sinusoidal shock is axially

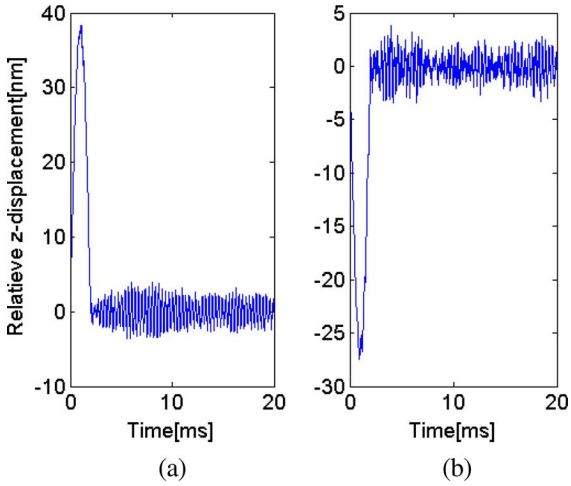

Fig. 21. Relative displacement (a) between top head and disk, and (b) between bottom head and disk.

TABLE III
MAXIMUM VARIATION OF THE FLYING HEIGHT DUE TO SHOCK AMPLITUDE WITH THE DURATION OF 2 ms

	150G	250G	350G
Top head-disk	16.440 nm	27.401 nm	38.361 nm
Bottom head-disk	-11.765 nm	-19.609 nm	-27.453 nm

applied to the four corners of the base plate. The shock amplitude of 1 G is set at 0.7 N in this simulation. The displacement of the head and disk is calculated by using the mode superposition with the lowest 130 modes. Fig. 20 shows the absolute displacement of the top head, the connecting point of the disk and the bottom head under the half-sinusoidal shock with the amplitude of 350 G and the duration of 2 ms. The displacements of the top and the bottom heads, the connecting point of the disk are almost synchronous in the micrometer range due to the high stiffness of air bearings. Fig. 21 shows the relative displacement between the top head and the disk, and between the bottom head and the disk. A head crash may take place when the relative displacement between disk and head is greater than the flying height. Table III show the maximum variation of the flying height between the disk and the top head and between the disk and the bottom head due to the variation of shock amplitude. It shows that the maximum variation of flying height increases with increasing shock amplitude.

IV. CONCLUSION

This paper proposes a finite-element method with mode superposition to analyze the shock response of a HDD composed of a spinning disk-spindle system with FDBs, a head-suspension-actuator with pivot bearings and air bearings, and a base plate with complicated geometry. Experimental testing shows that the proposed method accurately predicts the peak value of the vibration due to shock. It can be utilized to predict the operating shock response such as head crash in order to design a robust HDD.

REFERENCES

[1] D.-W. Shu, B.-J. Shi, H. Meng, F. F. Yap, D.-Z. Jiang, Q. Ng, R. Zambri, J. H. T. Lau, and C.-S. Cheng, "Shock analysis of a head actuator assembly subjected to half-sine acceleration pulses," *Int. J. Impact Eng.*, 2005.

[2] Q. H. Zeng and D. B. Bogy, "Numerical simulation of shock response of disk-suspension-slider air bearing systems in hard disk drives," *Microsyst. Technol.*, vol. 8, pp. 189–196, 2002.

[3] E. M. Jayson, J. M. Murphy, P. W. Smith, and F. E. Talke, "Shock and head slap simulations of operational and nonoperational hard disk drive," *IEEE Trans. Magn.*, vol. 38, no. 5, pp. 2150–2152, Sep. 2002.

[4] C. W. Tseng, J. Y. Shen, and I. Y. Shen, "Vibration of rotating-shaft HDD spindle motors with flexible stationary parts," *IEEE Trans. Magn.*, vol. 39, no. 2, pp. 794–799, Mar. 2003.

[5] G. H. Jang, J. H. Han, and C. H. Seo, "Finite element modal analysis of a spinning flexible disk-spindle system in a HDD considering the flexibility of complicated supporting structure," *Microsyst. Technol.*, vol. 11, pp. 488–498, 2005.

[6] G. H. Jang, C. H. Seo, and H. S. Lee , "Finite element modal analysis of an HDD considering the flexibility of spinning disk-spindle, head-suspension-actuator and supporting structure," *Microsyst. Technol.*, 2007, to be published.

[7] R. B. Lehoucq and D. C. Sorensen, "Deflation techniques for an implicitly restarted Arnoldi iteration," *J. Matrix Anal. Appl. SIAM*, pp. 789–821, 1996.

[8] A. K. Chopra, *Dynamics of Structures*, 3rd ed. Englewood Cliffs, NJ: Prentice-Hall, 2001, pp. 165–171.

Manuscript received December 15, 2006. Corresponding author: G. H. Jang (e-mail: ghjang@hanyang.ac.kr).